High-speed synthetic aperture microscopy for live cell imaging

Moonseok Kim,[1] Youngwoon Choi,[1] Christopher Fang-Yen,[2] Yongjin Sung,[3] Ramachandra R. Dasari,[3] Michael S. Feld,[3] and Wonshik Choi[1,*]

[1]*Department of Physics, Korea University, Seoul 136-701, South Korea*

[2]*Department of Bioengineering, University of Pennsylvania, Philadelphia, Pennsylvania 19104, USA*

[3]*G. R. Harrison Spectroscopy Laboratory, Massachusetts Institute of Technology, Cambridge, Massachusetts 02139, USA*

**Corresponding author: wonshik@korea.ac.kr*

Received October 22, 2010; revised November 30, 2010; accepted December 3, 2010; posted December 13, 2010 (Doc. ID 137048); published January 6, 2011

We present a high-speed synthetic aperture microscopy for quantitative phase imaging of live biological cells. We measure 361 complex amplitude images of an object with various directions of illumination covering an NA of 0.8 in less than one-thirteenth of a second and then combine the images with a phase-referencing method to create a synthesized phase image. Because of the increased depth selectivity, artifacts from diffraction that are typically present in coherent imaging are significantly suppressed, and lateral resolution of phase imaging is improved. We use the instrument to demonstrate high-quality phase imaging of live cells, both static and dynamic, and thickness measurements of a nanoscale cholesterol helical ribbon.

OCIS codes: 110.1650, 110.3175, 100.3175, 100.6950.

Interferometric microscopy techniques are capable of recording a complex light field. Compared to conventional phase microscopy techniques such as phase-contrast microscopy and differential-interference-contrast (DIC) microscopy, interferometric microscopy can quantify the phase change induced by the specimen. Many applications of the quantitatively recorded phase information have been reported in studying biological specimens [1,2]. For samples with a homogeneous refractive index, quantified phase information can be used to determine the height of samples with nanometer accuracy [3]. Another important use of phase information is that it enables high-speed three-dimensional (3D) imaging of a sample without scanning an objective lens via numerical propagation along the axial direction [4]. The quantitative phase microscopy techniques typically adopt spatially and temporally coherent sources (e.g., lasers) to facilitate both the phase recording and the numerical propagation. However, the use of coherent light sources has two important drawbacks. The first is the inferior spatial resolution of incoherent illumination owing to the small NA of the illumination [4]. A second drawback is the fixed pattern noise induced by diffraction from dust particles and other optical imperfections in the beam path and from the sample itself. When interpreting the acquired phase information as the thickness of a sample, such noise degrades the accuracy of the measurements.

We note that aperture synthesis methods can be used to increase the effective illumination NA without compromising the 3D imaging ability [5–7]. The concept of the aperture synthesis is to first record multiple electric field (E-field) images taken at several different angles of illumination covering different parts of an object spectrum, and then to synthesize them in such a way as to increase the passband of the object spectrum. Many studies have demonstrated the use of aperture synthesis to improve spatial resolution. However, most of the studies demand a long data acquisition time because of the need for rotating a sample or for changing the illumination, although a hybrid approach may reduce the number of images to be acquired [8].

In this work, we developed a high-speed synthetic aperture microscope for quantitative phase imaging of live biological cells. The experimental setup (Fig. 1) resembles that of our previous work [9] but with the sample illumination angle controlled by a dual-axis galvanometer-driven scanning mirror (Cambridge Technology) rather than a single-axis scanner. This allows the illumination to be varied in both the polar and azimuthal angles. In addition, we employ an off-axis digital holography method instead of phase-shifting interferometry to speed up the data acquisition. As a result, we could typically record 360 images in less than one-thirteenth of a second. For the aperture synthesis, a phase-referencing algorithm is developed to constructively add multiple angular images. We demonstrate quantitative phase imaging of live cells with aperture synthesis for the first time to our knowledge. Because of the increase in the passband, the lateral resolution

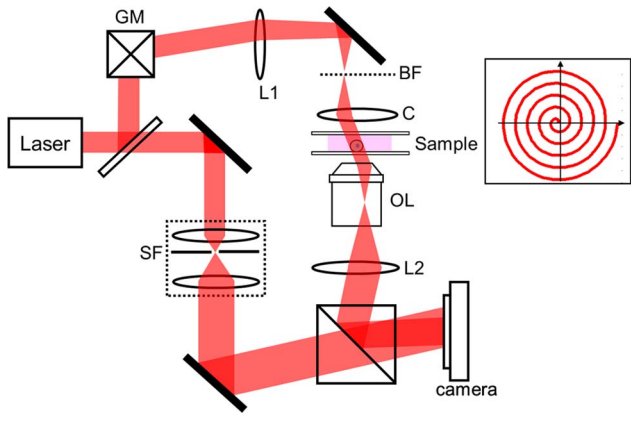

Fig. 1. (Color online) High-speed synthetic aperture phase microscopy setup. Laser: He–Ne laser; GM, dual-axis galvanometer scanning mirror; L1, $f = 250$ mm lens; BF, backfocal plane of condenser lens; C, condenser lens; OL, objective lens; L2, tube lens; SF, spatial filter system. Inset, spiral trajectory of the focused spot at BF.

is improved and the phase sensitivity is enhanced via a decrease in the depth of field [10].

The theory of aperture synthesis has been described in detail elsewhere [5–7]. For a plane wave with oblique incidence, $U_{\text{in}} = \exp(-2\pi i(\nu_x x + \nu_y y))$, onto an object located at the front focal plane and whose amplitude transmittance is $t(x, y)$, the field at the backfocal plane of an objective lens is given as follows:

$$U_f(\xi,\eta) = \frac{1}{i\lambda f}\,\text{circ}\left(\sqrt{\frac{\xi^2+\eta^2}{\Delta\nu}}\right) T(\xi/\lambda f + \nu_x, \eta/\lambda f + \nu_y). \tag{1}$$

Here $T(\xi\lambda f, \eta\lambda f)$ is the Fourier transform of $t(x, y)$, circ function is introduced to represent the limited aperture of the imaging system, and $\Delta\nu = f \times \text{NA}$, with f the focal length of the lens. Note that the spectrum shift enables us to accept the high-frequency band when the incident field is oblique. Therefore, by synthesizing various illumination angles, we can effectively enlarge the passband and thus the NA.

In the experiment, we use an off-axis digital holography microscopy to record the phase and amplitude of light transmitted through biological cells [1,9]. The output of a He–Ne laser ($\lambda = 632.8\,\text{nm}$) is divided into sample and reference beams (Fig. 1). A dual-axis galvanometer mirror is positioned in the sample beam path to scan the direction of illumination. A lens (L1) and a high-NA condenser lens (Nikon, 1.4 NA) relay the reflected beam from the galvanometer mirrors onto the sample. The beam transmitted through the sample is imaged by a complementary metal-oxide semiconductor camera (RedLake M3, 500 fps, or Photron 1024PCI, 5000 fps) using an objective lens (Olympus UPLSAPO 100X, 1.4 NA) and a tube lens. In the reference beam path, the beam is spatially filtered and expanded to match the mode with the sample beam. A beam splitter combines the sample and reference beams to form an interferogram at the camera.

To uniformly cover the NA of the condenser lens, we control the dual-axis galvanometer mirrors such that the beam spot at the back focal plane of the condenser lens moves along a spiral pattern with five rotations as shown in the inset of Fig. 1. For a given angle of illumination, the camera records an off-axis hologram whose spatial fringe period is equal to the diffraction-limited resolution. This enables us to record a complex amplitude image with a single interferogram, instead of four as in the previous phase-shifting interferometry. In doing so, we eliminate the required dwelling time of the galvanometer mirror for taking four images at a given angle and greatly improve data acquisition speed. By using a Hilbert transform, we obtain both phase and amplitude of the field and constructed E-field.

To increase the NA of the illumination, we synthesize a set of E-field images obtained at various angles of illumination. For illumination parallel to the optic axis of the objective lens, the phase image has a uniform background [Fig. 2(a)]. Here, the sample is a live microglia cell sandwiched between coverslips. By taking the Fourier transform of the E-field, we obtain the intensity distribution in the Fourier plane [Fig. 2(e)]. The center of the peak in the Fourier plane is due to the unscattered light, which we call a DC spot. The red circle indicates the limit of the passband with its radius corresponding to the spatial frequency $\text{NA}_{\text{obj}}/\lambda$, where NA_{obj} is the NA of the objective lens. For any nonzero degree of illumination, there is a linear phase ramp in the image plane as seen in Fig. 2(d). This causes the DC spot in the Fourier plane to be shifted away from the center while the passband (red circle) remains fixed.

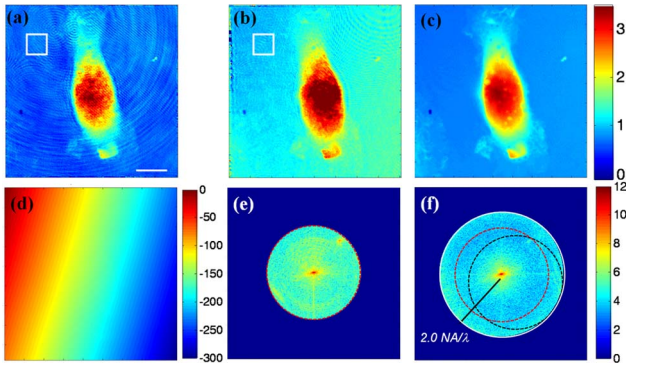

Fig. 2. (Color online) Angular images and synthesized images for a live microglia cell. (a), (d) Phase images taken in the image plane with illumination angles of 0° and 23.3°, respectively. (b) Phase image after background subtraction. (c) Phase image after aperture synthesis. Media 1 shows the dynamics of ruffles taken by the synthetic aperture quantitative phase microscopy. It takes one-fifth of a second to record one synthesized image, which is composed of 100 angle-dependent images taken at 500 frames per second. The cell is observed for 10 min. (e), (f) Intensity distribution in the Fourier plane for 0° illumination and for aperture synthesis, respectively. Color bars indicate phase in radians, and intensity in the logarithmic scale with base 10 for (e) and (f). Scale bar, 10 μm.

We now describe our method of synthesizing multiple angle-dependent images. In the previous studies, the DC spot of nonzero degree illumination is shifted to the center in the Fourier plane. In our approach, we combine images at the image plane. For this, we normalize the E-field image with a background image taken in the absence of the sample [Fig. 2(b)]. Then, the phase ramp is removed and the DC spot moves to the center in the Fourier plane. This causes the circle defining the passband (red circle) to shift away from the center of the Fourier map [black circle in Fig. 2(f)]. By repeating the same procedure for all the angular images, the passband is enlarged (white circle). As a result, the synthesized NA is increased from 1.4 [Fig. 2(e)] to 2.0 [Fig. 2(f)].

The advantage of synthesizing images at the image plane is in matching relative phase among angular images. Interferometric imaging is subject to the overall phase fluctuation from one recording to another due to path-length fluctuation between sample and reference. This is often referred to as an uncontrollable phase shift. When adding the set of angular images, it is important to eliminate the overall phase fluctuation, or the phase of the synthesized image will be lost. For example, the phase image in Fig. 2(b) has a nonzero phase at the background even after removing the phase ramp, which is different from that in Fig. 2(a) as a consequence of uncontrolled phase shift. We choose an area outside of

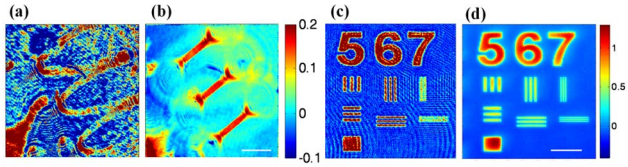

Fig. 3. (Color online) Images of a helical cholesterol ribbon [(a), (b)] and a USAF targetlike phase pattern [(c), (d)]. Phase images for angle of 0° illumination [(a), (c)] and for aperture synthesis [(b), (d)]. Media 2 is a movie showing the comparison between individual angular images on the left (panel a) and the synthesized image on the right (panel b). Color bars indicate phase in radians. Scale bar, 10 μm.

the specimen [white square boxes in Figs. 2(a) and 2(b)] and set the average phase of the area to be zero for all the E-field images by subtracting the measured average phase for each image. When we do so, the phase at the background is fixed for all the angular images. After adding all the E-field images, we obtain the phase image shown in Fig. 2(c). The fixed pattern diffraction noise present in the individual angular images is removed, and the overall rms phase noise is significantly reduced from 73 mrad to 16 mrad. This is a clear demonstration that aperture synthesis improves phase sensitivity. The enlarged passband leads to the reduction in the depth of field, which in turn rejects diffraction noise originating from the out-of-focus plane. The ruffles of the live microglia cell are clearly visible in Fig. 2(c) (Media 1), which indicates that the cell is alive because only vital cells can stretch their ruffles for moving.

With the improved phase sensitivity of our device, we image a helical cholesterol ribbon formed in surfactant mixtures [9]. A helical ribbon is an interesting object in that it may be used as a mesoscopic transducer to measure the forces on nanoscale biological objects. But the thickness needs to be measured to determine the spring constant of a ribbon. The typical thickness is smaller than 100 nm, well below the axial resolution of conventional microscopy. With a single angle phase image [Fig. 3(a)], however, diffractions from the object itself and particles in the medium contribute to the phase noise. On the other hand, the synthesized phase image [Fig. 3(b) (Media 2)] has dramatically reduced noise where the image shows the bottom part of a ribbon. Here, we record 361 angle-dependent images at 5000 frames per second. From the acquired phase, the thickness of the ribbon is determined to be 68 nm [9].

The spatial resolution of the phase image is also improved after the aperture synthesis. A United States Air Force (USAF) targetlike phase pattern is generated on a spatial light modulator (SLM) (Holoeye, LC-R 2500) with half pitch of the stripe patterns under numbers 5, 6, and 7 corresponding to 1200, 800, and 400 nm, respectively. To make small stripe patterns on the sample plane, the SLM is inserted at the conjugate plane to the sample plane and its pattern is demagnified by a factor of 50. Figure 3(c) is an averaged image of 1000 interferograms taken at 0° illumination, for which the diffraction-limited resolution is 550 nm ($1.22\lambda/1.4$). Diffraction noise appears and the smallest pattern is indistinguishable. By contrast, a combined image [Fig. 3(d)] by aperture synthesis covering 0.8 NA of illumination resolves the smallest pattern as a result of the enhanced resolution ($1.22\lambda/2.2 = 350$ nm).

In conclusion, we have developed a quantitative phase microscopy system that uses aperture synthesis to enhance both the spatial resolution and phase sensitivity for imaging live biological cells and other samples. With high-speed beam scanning and phase referencing at the image plane, we achieved synthetic aperture quantitative phase imaging with the highest speed and resolution to this point, and demonstrated static and dynamic live cell imaging. The enhanced phase sensitivity has enabled us to determine the thickness of a nanometer-scale 3D object such as a helical cholesterol ribbon. This technique will facilitate the use of quantitative phase microscopy in studying nanoscale dynamics of biological cells and determining the thickness of various phase objects with nanometer accuracy.

We acknowledge Jaisoon Kim at Myongji University for advice about the optical system. This research was supported by the Basic Science Research Program through the National Research Foundation of Korea (NRF), funded by the Ministry of Education, Science, and Technology (MEST) (grant number: 20100011286), and also by the National Institutes of Health (P41-RR02594-24).

References

1. C. Fang-Yen, S. Oh, Y. Park, W. Choi, S. Song, H. S. Seung, R. R. Dasari, and M. S. Feld, Opt. Lett. **32**, 1572 (2007).
2. B. Rappaz, P. Marquet, E. Cuche, Y. Emery, C. Depeursinge, and P. Magistretti, Opt. Express **13**, 9361 (2005).
3. B. Khaykovich, N. Kozlova, W. Choi, A. Lomakin, C. Hossain, Y. Sung, R. R. Dasari, M. S. Feld, and G. B. Benedek, Proc. Natl. Acad. Sci. USA **106**, 15663 (2009).
4. J. W. Goodman, *Introduction to Fourier Optics* (Roberts, 2005).
5. G. Indebetouw, Y. Tada, J. Rosen, and G. Brooker, Appl. Opt. **46**, 993 (2007).
6. C. J. Schwarz, Y. Kuznetsova, and S. R. J. Brueck, Opt. Lett. **28**, 1424 (2003).
7. T. Gutzler, T. R. Hillman, S. A. Alexandrov, and D. D. Sampson, Opt. Lett. **35**, 1136 (2010).
8. R. Fiolka, K. Wicker, R. Heintzmann, and A. Stemmer, Opt. Express **17**, 12407 (2009).
9. W. Choi, C. Fang-Yen, K. Badizadegan, S. Oh, N. Lue, R. R. Dasari, and M. S. Feld, Nat. Methods **4**, 717 (2007).
10. M. Debailleul, B. Simon, V. Georges, O. Haeberle, and V. Lauer, Meas. Sci. Technol. **19**, 074009 (2008).